

Occupation-constrained interband dynamics of a non-hermitian two-band Bose-Hubbard Hamiltonian

Manuel H. Muñoz-Arias,¹ Carlos A. Parra-Murillo,¹ Javier Madroño,^{1,2} and Sandro Wimberger^{3,4,5}

¹*Departamento de Física, Universidad Del Valle, A. A. 25360, Cali, Colombia*

²*Centre for Bioinformatics and Photonics-CIBioFi,*

Calle 13 No. 100-00, Edificio 320, No. 1069, Cali, Colombia

³*Dipartimento di Scienze Matematiche, Fisiche e Informatiche,*

Università di Parma, Parco Area delle Scienze 7/a, 43124 Parma, Italy

⁴*INFN, Sezione di Milano Bicocca, Gruppo Collegato di Parma, Parma, Italy*

⁵*ITP, Heidelberg University, Philosophenweg 12, 69120 Heidelberg, Germany*

(Dated: November 7, 2018)

The interband dynamics of a two-band Bose-Hubbard model is studied with strongly correlated bosons forming single-site double occupancies referred to as doublons. Our model for resonant doublon interband coupling exhibits interesting dynamical features such as quantum Zeno effect, the generation of states such as a two-band Bell-like state and an upper-band Mott-like state. The evolution of the asymptotic state is controlled here by the effective opening of one or both of the two bands, which models decay channels.

PACS numbers: 05.45.Mt, 03.65.Xp, 03.65.Aa, 05.30.Jp

I. INTRODUCTION

The Bose-Hubbard (BH) Hamiltonian is a celebrated many-particle model describing atoms trapped in a periodic array of potential wells [1]. The simplest version of this model, the single-band Bose-Hubbard Hamiltonian, already accounts for a plethora of interesting physical phenomena which have been investigated in experiments with ultracold quantum gases and optical lattices formed by laser beam interference patterns [2]. These setups provide a high degree of system control as, for instance, of the lattice depth that rules the inter-well particle tunneling, and of interparticle interaction tuned via Feshbach resonances [2]. The combination of this two components permits the implementation of the remarkable idea of quantum simulation that allows for the understanding of the underlying physics of complex systems in a clean manner [2, 3]. However, a whole set of physical phenomena are left away within the single-band approach. An example is the Landau-Zener transitions reported in Refs. [4–6] and theoretically tackled using mean field methods [7]. Yet, the limit of strongly correlated particles is more challenging to treat since the Bose-Hubbard Hamiltonian extended to higher bands contains a lot of new single and many-particle processes rendering the system overwhelmingly complex [8, 9].

The effects of higher Bloch bands on the single-particle dynamics [10] and on the spectral statistics of the single-band approach [11] were studied. One may address the problem by restricting the Fock space to a two-band Bose-Hubbard Hamiltonian, where the interband coupling is induced via an external field [8, 9]. In this paper we are interested in the two-band Bose-Hubbard Hamiltonian assuming strong correlation between the particles constraining the single-site interband coupling to occur only when there is more than one particle in one site. Our constrained model, that allows only for specific interband

tunneling processes, is a special situation of the full two-band model recently studied in the different context of periodic driving [12].

We explore the dynamical possibilities arising from coupling the system to decay channels, e.g. corresponding to higher energy bands, which are neglected in our model. Thus, the effective "reservoir" consists of the continuum part of the Wannier-Stark spectrum [4, 5, 10]. Our motivation to explore the dynamics of an open two-band system is inspired by recent works reporting emergent phenomena induced by loss. Examples are the work on quasi-dissipation free subspaces of entangled atomic Bell-like states [12], localization of BECs via boundary dissipation [13], entanglement detection [14], the possibility of controlling many-body quantum dynamics by localized dissipation [15, 16]. Dissipation replaces the continuous observations required to observe a quantum Zeno effect [6, 17–20]. The engineering of controlled on-site dissipation channels has been developed in recent experiments [20, 21] such that the range of possible experimental applications is continuously increasing. Modern experimental methods may as well allow for addressing individual bands in a lattice by state-selective excitation processes, see e.g. [4]. This motivates the application of decay channels with independent rates in our system.

This work is organized as follows. In Sec. II, we introduce our constrained two-band BH model to study correlated interband dynamics. We also sketch how our model can be extracted from the full two-band BH model [9] and the specific set of interband phenomena it aims to represent. In Sec. III, we briefly present the methodology to study correlated interband dynamics. Sec. III A presents results regarding the emergence of the quantum Zeno effect in the interband transport, and the conditions under which it appears. In Sec. III B, we show how by controlling the ratio between the dissipation rates of the bands one can prepare interesting superposition states,

in particular those Bell-like states already found in [12]. Finally in Sec. IV we present a brief summary and conclusions of our work.

II. PHYSICAL SYSTEM AND HAMILTONIAN

Our Hamiltonian, see Eq. (1) below, is a restricted model of a much more complex system introduced and discussed, e.g., in our previous works [9, 12]. It has the great advantage that the complexity is much reduced taking into account only the dominant interband couplings under specific resonant tunneling conditions. The first part corresponds to two independent copies of the tilted single-band BH chain, with the external field with magnitude F defining the Wannier-Stark force. The second part describes interband coupling restricted to single-site occupation number, i.e., there will be transitions only if an individual site is occupied by more than one particle. The dynamics is induced by two transport processes: first, the intraband hopping of particles between next-neighboring sites, and second interband tunneling of so-called doublons [22–24]. Altogether, these processes are described by the following effective Hamiltonian:

$$\begin{aligned} \hat{H} = & \sum_{l, \alpha=\{a,b\}} \left[\varepsilon_l^\alpha \hat{n}_l^\alpha - \frac{J_\alpha}{2} (\hat{a}_{l+1}^\dagger \hat{a}_l + \text{H.c.}) + \frac{W_\alpha}{2} \hat{a}_l^{\dagger 2} \hat{a}_l^2 \right] \\ & + \sum_l \left[G_a \hat{b}_l^\dagger \hat{a}_l \hat{n}_l^a (\hat{n}_l^a - 1) + G_b \hat{a}_l^\dagger \hat{b}_l \hat{n}_l^b (\hat{n}_l^b - 1) + \text{H.c.} \right] \\ & + \sum_l W_x \hat{n}_l^a \hat{n}_l^b \end{aligned} \quad (1)$$

with

$$\varepsilon_l^\alpha = \left[d_L F l + \frac{\Delta_g}{2} (\delta_{\alpha,b} - \delta_{\alpha,a}) - i\Gamma_\alpha \right] \hat{n}_l^\alpha.$$

Here, $\alpha = a (b)$ refers to the lower (upper) band, $\hat{a}_l^\dagger (\hat{a}_l)$ are bosonic creation (annihilation) operators with J_α the hopping amplitude of each band, and \hat{n}_l^α the number operator. The on-site interparticle interaction strengths are W_α and Δ_g stands for the on-site energy bandgap. The interband coupling is represented by the G -terms. Such a coupling implies that only when there are more than one particle in a single site anywhere in the lattice one particle will be promoted to the other band. Its respective counterpart implies the increase of a single-site occupancy wherever there is at least one particle (see G_x process in Fig. 1-(a)). In the case of unitary filling condition for the lattice, i.e., $N/L = 1$ for any N , the most probable higher occupation of a single lattice site is a double occupancy, therefore, it is expected to get doublon-mediated interband dynamics. In addition, we have an external Stark field F that helps us to tune different resonant regimes [12].

In Fig. 1-(a) we present a scheme of the different processes considered in the effective model, and of those that

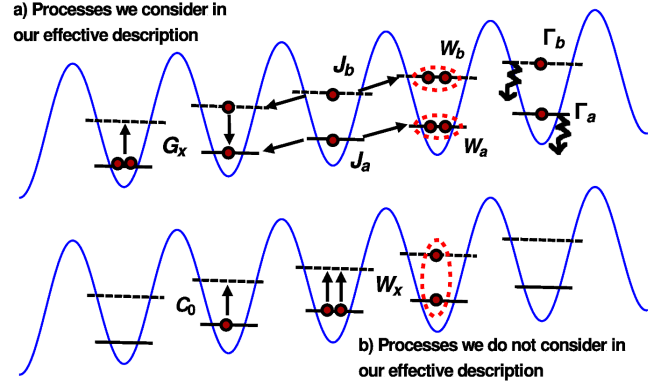


Figure 1: (Color online) (a) Representation of the different processes that take place under the Hamiltonian in Eq. (1). Particles can jump between next neighboring sites with an amplitude $J_{a,b}$, doubly or higher occupation of the lattice sites have an increment in energy proportional to $W_{a,b}$, the external field contributes with an increment in the energy proportional to the magnitude of the external field (F) and the position to the lattice. The inter-band transport occurs with an amplitude G_x , and $\Gamma_{a,b}$ stands for the decay rates of the two Bloch bands. (b) Usual complementary terms of the full two-band BH model [9] that we are not taking into account within our effective description. Notice that, under the regime of parameters we are working, these processes are well represented by the $G_{a(b)}$ term. Below we show, for instance, that including the W_x term almost does not affect the dynamics.

we do not take into account from the original full Hamiltonian (see Fig. 1-(b)). Note that the Hamiltonian \hat{H} is not hermitian since the unperturbed energies contain the imaginary number $-i\Gamma_\alpha$ representing the effective opening of the system, i.e., decay rates for every band. This implies that the eigensystem of \hat{H} consists of a set of eigenvalues of the form $\varepsilon_i = E_i - i\Gamma_i/2$ and metastable eigenstates with the lifetime $\tau_i \sim 1/\Gamma_i$.

A resonant tunneling between two- and single-particle levels is expected as a consequence of the interband G_x coupling term in Eq. (1). Here, there is no need for a time-dependent driving as in Ref. [12] and G_x is taken constant in what follows. We consider the following possibilities for the initial conditions for our time evolution:

- (i) $F_0 = W_a/2\pi$, $|\psi_0\rangle = |111\cdots; 000\cdots\rangle$,
- (ii) $F_0 = 0$, $|\psi_0\rangle = |2020\cdots, 000\cdots\rangle$.

The difference between the initial states is just the presence of the Stark field at $t = 0$. The two initial states can be dynamically connected by the hopping term [23, 24], hence the time evolution is expected to be equivalent, if not the same. We consider decay rates $\Gamma_\alpha \ll J_\alpha$, where $J_\alpha \ll \{U_\alpha, \Delta_g\}$. This means that decay is slow and the total particle number tends to be preserved with high probability. Then our effective Hamiltonian approach is a good approximation to more complex master equation approaches, see e.g. [25, 26].

In all numerics we compute the time evolution operator

$\hat{U}_t = \hat{\mathcal{T}} \exp \left[-i \int_0^t \hat{H}(t') dt' \right]$. With the help of \hat{U}_t , we compute the time-evolved many-body state starting from a given initial state $|\psi_0\rangle$. The figure of merit to study the interband dynamics is the population inversion, i.e., the population imbalance between the bands defined by

$$M_t = \langle \psi_t | \frac{1}{N} \sum_l (\hat{n}_l^b - \hat{n}_l^a) | \psi_t \rangle / \langle \psi_t | \psi_t \rangle. \quad (2)$$

Our study is divided in two parts. We first consider the situation in which only the upper Bloch band is open, i.e., $\Gamma_a = 0$ and $\Gamma_b \neq 0$. In this limit, it will be shown that quantum Zeno-like dynamics occurs induced by the dissipative process during the promotion of particles to the upper band. Secondly, we explore the dynamical consequences of simultaneously opening both Bloch bands what results in the formation of a Bell-like state.

III. NUMERICAL RESULTS

A. Quantum Zeno effect in the inter-band dynamics

A quantum system prepared in a meta-stable state can be dynamically locked/frozen by means of continuous observations [17, 20] or by the control of the system via temperature and entropy [27]. This phenomenon, known as quantum Zeno effect, is a paradigm of the measurement process in quantum mechanics. We now show how the quantum Zeno effect occurs in our system thus changing radically the expected interband transport (See Refs. [8]).

Let us start considering the decay rates only in the upperband, i.e., $\Gamma_b \neq 0$ and $\Gamma_a = 0$, and the system defined by the filling factor $N/L = \{2/2, 4/4\}$ corresponding to N particles in L lattice sites. The initial state is taken as the lower-band Mott state $|111\cdots; 000\cdots\rangle$ which is dynamically evolved with a fixed tilting $F_0 = W_a/2\pi$ ensuring the resonant activation of the interband dynamics. This occurs in a time scale in which many hopping processes are allowed, leading to occasional double occupancies (doublons) in the lower band. Let g be the dissipation control parameter, i.e. $\Gamma \propto g$. In Fig. 2-(b) we see that the interband dynamics shows collapses and revivals for $g = 0$ at certain times, similar to those predicted in Ref. [8]. Here we have neglected the interband coupling term G_b since it does not change relevantly the results of this section. Yet, setting $g \neq 0$ we see that the role of the dissipation is to freeze the dynamics and the initial state, $|111\cdots; 000\cdots\rangle$, is asymptotically recovered (see Fig. 3). We stress that our Hamiltonian, see the sketch in Fig. 1, couples both bands, and that the decay occurs from both bands to outside the system. Hence, the observed suppression of upper-band population is non trivial. Indeed, it reflects nothing but the onset of the quantum Zeno effect [6, 17–19].

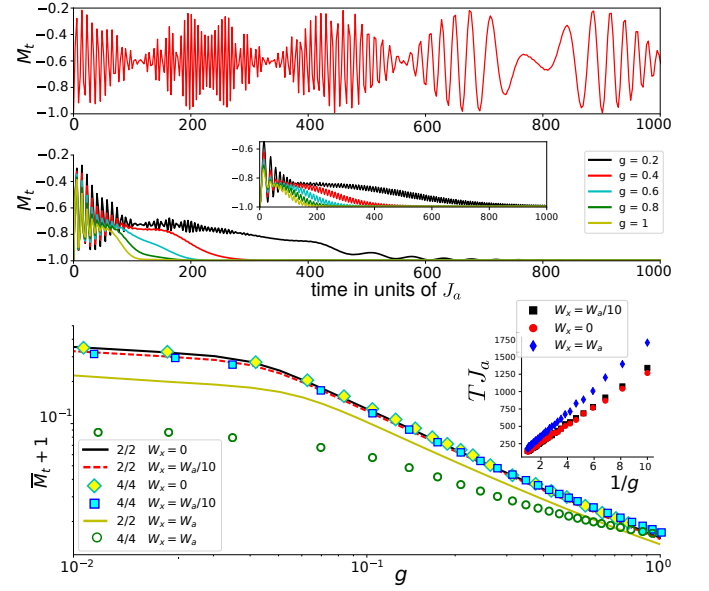


Figure 2: (Color Online) (a) Time evolution of the population inversion M_t for a closed system $\Gamma_a = \Gamma_b = 0$. (b) M_t for different values of Γ_b , we have taken $\Gamma_b = g \times 0.8 \times 10^{-3}$, with g a control parameter. We see a fast decay of M_t as we increase g , in all the cases the system ends in the state $|11; 00\rangle$. (c) Long time average of M_t as a function of g . We have plotted this curve in log-log scale after shifting \bar{M}_t by one. The red-continuous line is for the $N/L = 2/2$ system and the black-dotted line for the $N/L = 4/4$ system. The tale of both curves follows a power law, evidence of the quantum Zeno effect. The inset presents the decay time T of M_t as function of $1/g$, the linear behavior is evident. In addition we include the term containing the interparticle interaction between particles in different bands with intensity W_x to show that the results are practically the same, see for instance: red-dashed line, light-blue squares. In all the computations we use the BH parameters: $J_a = -J_b = 0.006$, $W_a = W_b = 0.034$, $W_x \approx (0.1 \dots 1) \times W_a$, $\Delta_g = 0.108$, $G_a = 0.09$ and $G_b = 0$.

To see this in a clean way, we compute the long-time average of M_t defined as $\bar{M}_t = \lim_{\tau \gg 1/|J_a|} \int_0^\tau M_t dt' / \tau$. In Fig. 2-(c) we plot \bar{M}_t as a function of the dissipation strength g (continuous line). The tail of this curve follows a power-law decay $\bar{M}_t \propto g^{-1}$. Note that this behavior is preserved even in the present of the interband coupling term: $W_x \sum_l \hat{n}_l^a \hat{n}_l^b$, (see panel Fig.1-(b)) where $W_x = (0.1 \dots 1) \times W_a$. Additionally, the inset shows the decay time T of the signal \bar{M}_t as a function of $1/g$, with a linear growth of $T \propto 1/g$, a clear signature of the quantum Zeno effect [14, 18]. The dots in Fig. 2-(c) correspond to the results for $N/L = 4/4$. We can see that the effect is still preserved for larger system sizes. In Fig. 3, we show how the initial condition, the Mott state $|111\cdots; 000\cdots\rangle$, is dynamically recovered after some time. For short, we initialize the system one step forward, that is, we directly evolve states with double occupancies $|2020\cdots; 0000\cdots\rangle$. Note that including the term W_x just delays the effect rather than washing

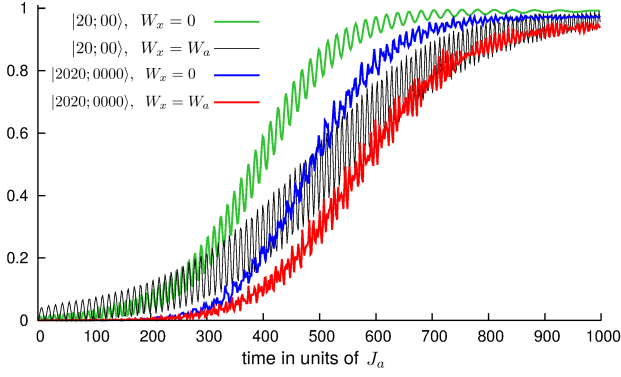


Figure 3: (Color Online) *Asymptotic state*: The figure shows the projection probability on the lower-band Mott state $|111\cdots; 000\cdots\rangle$ in time where it can be seen that it asymptotically grows to one as mentioned in the main text. The time evolution is computed for initial states of the type (main panel) $|2020\cdots; 0000\cdots\rangle$. The parameters are the same as in Fig.2 above; the W_x values are given in the legend.

it out.

B. Asymptotical dynamics: two-band Bell-like state and upper-band Mott state

To constrain the dynamics of a quantum system to a convenient subspace of the full Hilbert space is one of the hardest but, nevertheless, interesting open problems in quantum control theory. Besides, dissipation has always been related to the onset of decoherence which induces a strong mixing of a large number of accessible states. Yet, there have been advances towards quantum control by means of controlled dissipation processes, see e.g. [14, 16, 26]. This has found applications in the emerging field of atomtronics [28, 29].

Here, we show how the asymptotic dynamics governed by Eq. (1). First, we study the case $G_b = 0$ that yields a steady state with a structure resembling a Bell state. Secondly, we show that including $G_b \neq 0$, the asymptotic state takes the shape of a Mott state in the upper band. The latter result gives a possible way of creating such states.

To start, we evolve a lower-band Mott state for different ratios of the dissipation rates of every band $g \equiv \Gamma_a/\Gamma_b$. In Fig. 4-(a) main panel, we present the results for the minimal system $N/L = 2/2$. We see that for values of $g > 1$, M_t approaches zero in two steps. Firstly, it goes to $M_t \approx -0.2$ oscillating rapidly, and then after a time interval M_t reaches (smoothly) the interband balance population value $M_t \approx 0$. At this point, the resulting asymptotic state takes the form $|\psi_{t \gg 1/|J_a|}\rangle = \frac{1}{\sqrt{2}}(|10; 01\rangle + e^{i\phi_t}|01; 10\rangle)$, at which the dynamics remains frozen. This kind of state is also seen in the full model studied in Ref. [12]. There it was associated with a symmetry related to the inversion of the on-site population

of the bands. The structure of the $|\psi_{t \gg 1/|J_a|}\rangle$ resembles a Bell state.

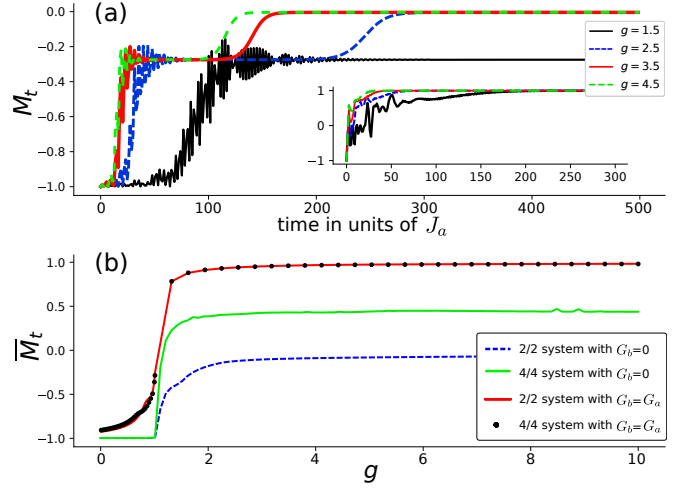


Figure 4: (Color Online) (a) The main panel shows the time evolution of the population inversion for the 2/2 system, with $\Gamma_b = 0.8 \times 10^{-3}$ and $\Gamma_a = g \times 0.8 \times 10^{-3}$. For values of $g > 0$ the initially locked state $|11; 00\rangle$ evolves toward the Bell-like state $|\psi_{\text{Bell}}\rangle = \frac{1}{\sqrt{2}}(|10; 01\rangle + |01; 10\rangle)$. The larger the value of g the faster we reach $|\psi_{\text{Bell}}\rangle$. The inset shows the results taking the G_x -terms into account with $G_b = G_a = 0.09$. We see that the saturation is no longer about $\bar{M}_t \rightarrow 0$ but $\bar{M}_t \rightarrow 1$, which implies that the asymptotic state is no longer of the Bell type but a Mott state $|\psi_{\text{Mott}}\rangle = |00; 11\rangle$. (b) Longtime average of M_t as a function of g . The BH parameters are the same as in Fig. 2. For the 2/2 system (dashed line), we reach a saturation point at $\bar{M}_t \approx 0$. However, for 4/4, the system (green line) reaches the saturation point at $\bar{M}_t \approx 0.5$, and the final state is a superposition dominated by the state $|1000; 2010\rangle$. When $G_b = G_a$, $\bar{M}_t \approx 1$ in the 2/2 system (red line) and in the 4/4 system (circles). By inspection we find that the asymptotic state takes the form of an upper-band Mott state in these cases.

Following [12], this association becomes clearer when transforming the Fock basis to a new picture therein called the w_l -representation. It follows that we can construct new states that have the form $|w_1 \cdots w_L\rangle$, with $w_l = n_l^b - n_l^a \in [-N, N]$. Therefore, the asymptotic state can be uniquely written as

$$\begin{aligned} |\psi_{t \gg 1/|J_a|}\rangle &= \frac{1}{\sqrt{2}}(|10; 01\rangle + e^{-i\phi_t}|01; 10\rangle) \\ &= \frac{1}{\sqrt{2}}(|+1; -1\rangle + e^{-i\phi_t}|-1; +1\rangle), \end{aligned} \quad (3)$$

with the phase factor obtained from the numerics. This notation is only helpful if the states involved in the dynamics fulfill the condition $n_l^a + n_l^b = 1$. The Bell-like structure of the state clearly appears and we can ensure that the asymptotic state is maximally entangled. The inclusion of the W_x -term does not change the shape of the asymptotic state but the transient dynamics, i.e., the stabilization time as the previous section.

In the case $G_b = G_a \neq 0$, that is, when the interband coupling from the upper to lower band is similarly constrained as for the reverse process, the asymptotic state is given by a Mott-like state in the upper band, i.e., $|\psi_{t \gg 1/|J_a|}\rangle \sim |000 \dots; 111 \dots\rangle$. Note that, since this also happens under the condition $\Gamma_a > \Gamma_b$, the upper band Mott state is the most stable state possible in the asymptotic regime. Here, no G_x -coupling will produce a transition between the bands because at least one doublon in the upper band has to be dynamically created. However, higher single site occupation will be removed rapidly by the dissipation. In the inset of Fig. 4(b) we show the saturation of the population inversion in time, which goes to $\bar{M}_t \rightarrow 1$ for the case $G_a = G_b$. After numerical inspection of the expansion coefficients, in both cases, i.e. $N/L = \{2/2, 4/4\}$, the asymptotic state is $|\psi_{t \gg 1/|J_a|}\rangle \approx |000 \dots; 111 \dots\rangle$.

In Fig. 4(b) we plot the average value of \bar{M}_t for $N/L = 2/2$ (black line) and $N/L = 4/4$ (green line) with and without the G_b -coupling term. The Mott state is still locked by the Zeno effect when $g \in [0, 1]$ while for $g > 1$ the interband dynamics is no longer prohibit, i.e., Zeno dynamics is no longer seen. For $N/L = 4/4$, the saturation values for \bar{M}_t is far from the perfect interband balance $\bar{M}_t = 0$ and the final superposition state is mainly dominated by the state $|1000; 2010\rangle$. Despite that there is still entanglement in the system, it is difficult to see a relevant structure of the asymptotic state in contrast to what is found in Ref. [12]. However, if $G_b \neq 0$ the upper-band Mott state continues to show up for $N/L = 4/4$.

IV. CONCLUSIONS

We presented an effective Hamiltonian model for a two-band BH system in the presence of correlated interband

tunneling processes. Our model accounts for the regime in which the doublon formation in the bottom band induces interband transport. Motivated by some recent results on quantum many-body systems [25], we opened the system, to explore the interband dynamics. With this model, we built an scheme for the preparation of superposition states. Additionally, we found that for the smallest non-trivial system our scheme allows us to drive the system towards a state that resembles a Bell state in the case of strongly constrained interband coupling from the lower to the upper band, while if both direction in the interband coupling are equally constrained, an upper-band Mott state occurs in the asymptotic dynamics. We presented signals of frozen quantum dynamics in a partially opened system, that is, top band open, bottom band closed, and we were able to relate that with the quantum Zeno effect in interband transport, see also [6]. The interband dynamics can be unfrozen by the controlled opening also of the bottom band. Finally, we have shown that the quantum Zeno effect in the interband dynamics still appears for larger systems.

V. ACKNOWLEDGMENTS

The authors acknowledge financial support of the University del Valle (project CI 7996). C. A. Parra-Murillo gratefully acknowledges financial support of COLCIENCIAS (grant 656), J.M. support from the Colombian Science, Technology and Innovation fund (Fondo CTEI-Sistema General de Regalías, contract BPIN 20113000100007) and COLCIENCIAS contract No. 71003, and S.W. support by the FIL2014 program of Parma University.

-
- [1] D. Jaksch, C. Bruder, J. Cirac, C. Gardiner, and P. Zoller, *Phys. Rev. Lett.* **81**, 3108 (1998).
 - [2] I. Bloch, J. Dalibard, and W. Zwerger, *Rev. of Mod. Phys.* **80**, 885 (2008); I. Bloch, J. Dalibard, and S. Nascimbène, *Nat. Phys.* **8**, 267 (2012).
 - [3] R. Islam, R. Ma, P. M. Preiss, M. E. Tai, A. Lukin, M. Rispoli, and M. Greiner, *Nature* **528**, 77 (2015); A. M. Kaufman, M. E. Tai, A. Lukin, M. N. Rispoli, R. Schittko, P. M. Preiss, and M. Greiner, *Science* **353**, 794 (2016).
 - [4] C. Sias, A. Zenesini, H. Lignier, S. Wimberger, D. Ciampini, O. Morsch, and E. Arimondo, *Phys. Rev. Lett.* **98**, 120403 (2007); C. Weitenberg, M. Endres, J. F. Sherson, M. Cheneau, P. Schauß, T. Fukuhara, I. Bloch, S. Kuh, *Nature* **471**, 319 (2011).
 - [5] A. Zenesini, H. Lignier, G. Tayebirad, J. Radogostowicz, D. Ciampini, R. Mannella, S. Wimberger, O. Morsch, and E. Arimondo, *Phys. Rev. Lett.* **103**, 090403 (2009); G. Tayebirad, A. Zenesini, D. Ciampini, R. Mannella, O. Morsch, E. Arimondo, N. Lörch, and S. Wimberger, *Phys. Rev. A* **82**, 013633 (2010).
 - [6] N. Lörch, F.V. Pepe, H. Lignier, D. Ciampini, R. Mannella, O. Morsch, E. Arimondo, P. Facchi, G. Florio, S. Pascazio, and S. Wimberger, *Phys. Rev. A* **85**, 053602 (2012).
 - [7] S. Wimberger, R. Mannella, O. Morsch, E. Arimondo, A. R. Kolovsky, and A. Buchleitner, *Phys. Rev. A* **72**, 063610 (2005).
 - [8] P. Plötz, P. Schlagheck, and S. Wimberger, *Eur. Phys. J. D* **63**, 47 (2011); P. Plötz, J. Madroñero, and S. Wimberger, *J. Phys. B.* **43**, 08001(FTC) (2010).
 - [9] C. A. Parra-Murillo, J. Madroñero, and S. Wimberger, *Phys. Rev. A* **88**, 032119 (2013); *Phys. Rev. A* **89** (5), 053610 (2014); *Annalen der Physik* **527**, 656 (2015); C. A. Parra-Murillo, *Ph.D. Thesis*, Heidelberg University (2013).
 - [10] M. Glück, A. R. Kolovsky, and H. J. Korsch, *Phys. Rep.* **366**, 103 (2002); D. N. Maksimov, E. N. Bulgakov, and

- A. R. Kolovsky, Phys. Rev. A **91**, 053631 (2015).
- [11] A. Tomadin, R. Mannella, and S. Wimberger, Phys. Rev. Lett. **98**, 130402 (2007); Phys. Rev. A **77**, 013606 (2008).
 - [12] C. A. Parra-Murillo, M. H. Muñoz-Arias, J. Madroño, and S. Wimberger, preprint arXiv:1611.06369 (2016).
 - [13] R. Livi, R. Franzosi, and G.-L. Oppo, Phys. Rev. Lett. **97**, 060401 (2006); R. Franzosi, R. Livi, and G.-L. Oppo, J. Phys. B **40**, 1195 (2007).
 - [14] P. Barmettler and C. Kollath, Phys. Rev. A **84**, 041606 (2010).
 - [15] V. A. Brazhnyi, V. V. Konotop, V. M. Pérez-García, and H. Ott, Phys. Rev. Lett. **102**, 144101 (2009); G. Barontini, R. Labouvie, F. Stubenrauch, A. Vogler, V. Guarrera, and H. Ott, Phys. Rev. Lett. **110**, 035302 (2013).
 - [16] D. Witthaut, F. Trimborn, and S. Wimberger, Phys. Rev. Lett. **101**, 200402 (2008); G. Kordas, S. Wimberger, and D. Witthaut, Phys. Rev. A **87**, 043618 (2013); G. Kordas, D. Witthaut, P. Buonsante, A. Vezzani, R. Burioni, A. I. Karanikas, and S. Wimberger, EPJ Spec. Topics **224**, 2127 (2015).
 - [17] B. Misra and E. C. G. Sudarshan, J. Mat. Phys. **18**, 756 (1977).
 - [18] A. G. Kofman and G. Kurizki, Nature **405**, 546 (2000).
 - [19] D. Witthaut, F. Trimborn, H. Hennig, G. Kordas, T. Geisel, and S. Wimberger, Phys. Rev. A **83**, 063608 (2011); Falchi P. and Pascazio S., J. Phys. A: Math. Theor. **41** 493001 (2008); Eur. Phys. J. D **63**, 63 (2011); Raizen M. G., Wilkinson S. R., Bharucha C. F., Fischer M. C., Madison K. W., Morrow P. R., Niu Q., Sundaram, B. Nature. **387** (6633), 575 (1997);
 - [20] D. A. Zezyulin, V. V. Konotop, G. Barontini, and H. Ott, Phys. Rev. Lett. **109**, 020405 (2012); R. Labouvie, B. Santra, S. Heun, and H. Ott, Phys. Rev. Lett. **116**, 235302 (2016).
 - [21] P. Würtz, T. Langen, T. Gericke, A. Koglbauer, and H. Ott, Phys. Rev. Lett. **103**, 080404 (2009).
 - [22] F. Meinert, M. J. Mark, E. Kirilov, K. Lauber, P. Weinmann, A. J. Daley, and H.-C. Nägerl, Phys. Rev. Lett. **111**, 053003 (2013); F. Meinert, M. J. Mark, E. Kirilov, K. Lauber, P. Weinmann, M. Gröbner, A. J. Daley, and H.-Ch. Nägerl, Science **344**, 1259 (2014); A. R. Kolovsky and D. N. Maksimov, Phys. Rev. A **94**, 043630 (2016).
 - [23] S. Sachdev, K. Sengupta, and S. Girvin, Phys. Rev. B **66**, 075128 (2002).
 - [24] A. R. Kolovsky, Phys. Rev. A **70**, 015604 (2004).
 - [25] G. Kordas, D. Witthaut, and S. Wimberger, Ann. Phys. **527**, 619 (2015).
 - [26] A. J. Daley, Adv. Phys. **63**, 77 (2014); M. B. Plenio and P. L. Knight, Rev. Mod. Phys. **70**, 101 (1998).
 - [27] N. Erez, G. Gordon, M. Nest, and G. Kurizki, Nature **452**, 724 (2008).
 - [28] A. Micheli, A. J. Daley, D. Jaksch, and P. Zoller, Phys. Rev. Lett. **93**, 140408 (2004); L. Amico, A. Osterloh, and F. Cataliotti, Phys. Rev. Lett. **95**, 063201 (2005); B. T. Seaman, M. Krämer, D. Z. Anderson, and M. J. Holland Phys. Rev. A **75**, 023615 (2007); A. Ivanov, G. Kordas, A. Komnik, and S. Wimberger, Eur. Phys. J. B **86**, 345 (2013).
 - [29] J.-P. Brantut, J. Meinike, D. Stadler, S. Krinner, and T. Esslinger, Science **337**, 1069 (2012); S. Eckel, J. G. Lee, F. Jendrzejewski, N. Murray, C. W. Clark, C. J. Lobb, W. D. Phillips, M. Edwards, and G. K. Campbell, Nature **506**, 200 (2014); S. Krinner, D. Stadler, D. Husmann, J.-P. Brantut, and T. Esslinger, Nature **517**, 64 (2015); R. Labouvie, B. Santra, S. Heun, S. Wimberger, and H. Ott, Phys. Rev. Lett. **115**, 050601 (2015).